necessary to clarify the detail of the problem.

Acknowledgment. We are greatly indebted to Dr. B. Gabrys for valuable discussion and comments. The financial supports of the Science and Engineering Research Council (U.K.) to this experiment and of the Japan Society for the Promotion of Science and British Council to T.K. are greatly appreciated.

Registry No. PSSNa, 9080-79-9; neutron, 12586-31-1.

References and Notes

(1) Neirlich, M.; Williams, C. E.; Boué, F.; Cotton, J. B.; Daudo, M.; Farnoux, B.; Jannink, G.; Picot, C.; Moan, M.; Wolf, C.; Rinaudo, M.; de Gennes, P.-G. *J. Phys. (Orsay, Fr.)* **1979**, *40*, 701.
(2) Nierlich, M.; Boué, F.; Lapp, A.; Oberthür, R. *Colloid Polym. Sci.* **1985**, *263*, 955.
(3) Nierlich, M.; Boué, F.; Lapp, A.; Oberthür, R. *J. Phys. (Orsay, Fr.)* **1985**, *46*, 649.
(4) Kaji, K.; Urakawa, H.; Kanaya, T.; Kitamaru, R. *Macromolecules* **1984**, *17*, 1835.
(5) Kaji, K.; Urakawa, H.; Kanaya, T.; Kitamaru, R. *J. Phys. (Orsay, Fr.)* **1988**, *49*, 993.
(6) Gruner, F.; Lehmann, W. P.; Fahlbusch, H.; Weber, R. *J. Phys. A: Math. Gen.* **1981**, *14*, L307.
(7) Drifford, M.; Dalbirz, J. P. *J. Phys. Chem.* **1984**, *88*, 5368.
(8) de Gennes, P.-G.; Pincus, P.; Velasca, R. M.; Brochard, F. *J. Phys. (Orsay, Fr.)* **1976**, *37*, 1461.
(9) Odijk, T. *Macromolecules* **1979**, *12*, 1461.
(10) Le Bret, M. *J. Chem. Phys.* **1982**, *76*, 6243.
(11) Hayter, J.; Jannink, G.; Brochard-Wyart, F.; de Gennes, P. G. *J. Phys. Lett. (Orsay, Fr.)* **1980**, *41*, L-451.
(12) Nallet, F.; Jannink, G.; Hayter, J.; Oberthür, R.; Picot, C. *J. Phys. (Orsay, Fr.)* **1983**, *44*, 87.
(13) Nyström, B.; Roots, J.; Higgins, J. S.; Gabrys, B.; Peiffer, D. G.; Mezei, F.; Sarkissian, B. J. *J. Polym. Sci., Polym. Lett. Ed.* **1986**, *24*, 273.
(14) Neutron Spin Echo. *Lecture Note in Physics*; Mezei, F., Ed.; Springer-Verlag: Berlin, 1980; Vol. 128.
(15) Perrin, F. *J. Phys. Radium VII* **1934**, *5*, 497. Perrin, F. *J. Phys. Radium VII* **1936**, *7*, 1. Koenig, S. H. *Biopolymers* **1975**, *14*, 2421. It should be noted that the formulas for the orientational relaxation times of ellipsoids in the original paper of Perrin were corrected by Koenig. However, the formula for the translational diffusion which was used in the present calculation is not incorrect in the original paper of Perrin.
(16) Kaji, K.; Urakawa, H.; Kanaya, T.; Kitamaru, R., unpublished data.

Anisotropic Counterion Polarizations and Their Dynamics in Aqueous Polyelectrolytes As Studied by Frequency-Domain Electric Birefringence Relaxation Spectroscopy

Norio Ookubo,* Yoshinori Hirai, Kohzo Ito, and Reinosuke Hayakawa

Department of Applied Physics, Faculty of Engineering, University of Tokyo, Bunkyo-ku, Tokyo 113, Japan. *Received January 29, 1988; Revised Manuscript Received August 4, 1988*

ABSTRACT: Dielectric properties of polyelectrolyte solutions in a semidilute regime at low ionic strength were studied by means of frequency-domain electric birefringence (FEB) relaxation spectroscopy. The observed FEB spectra showed simultaneously three relaxations, two of which were assigned to the low-frequency (LF) and high-frequency (HF) relaxations already found in the dielectric relaxation spectroscopy. The remaining one in the lowest frequency was the orientational (rotational) relaxation of the polyion with an extended conformation. The LF relaxation distinct from the rotational one indicated that it arose from the counterion motion along the polyion axis with a slower mobility than that in a free medium. The HF relaxation, on the other hand, showed the birefringence sign opposite to that of the LF relaxation and hence it was attributed to the counterion motion perpendicular to the polyion axis. Thus, the LF and HF relaxations of polyelectrolyte solutions are regarded as manifestations of anisotropic motions of bound counterions relative to the extended polyion in the directions parallel and perpendicular to the polyion axis, respectively.

Introduction

A linear polyelectrolyte solution (polyion–counterion system) has long been an attractive subject for many researchers because of its peculiar properties[1-3] such as a strong dependence of the conformation of highly charged polyions on the ionic environment and an anomalous dielectric behavior due to the counterions in the vicinity of the polyions.

The polyion conformation has been theoretically analyzed in terms of the electrical persistence length L_e (i.e., the contribution of electrostatic forces to the persistence length) of the polyion by using Debye–Hückel[4-6] and Poisson–Boltzmann[7,8] formulations. These analyses have revealed that if the ionic strength determined by the concentrations of added salts and counterions dissociated from polyions is sufficiently low, L_e can be large enough to lead the polyion to an extended conformation. In high ionic strength, on the contrary, as in the case with excess amount of added salts, L_e would be reduced to a much smaller value and the polyion would be of a coiled form just like uncharged flexible polymers in solution.

Under low ionic strength, the polyions with large L_e entangle with each other more easily than uncharged flexible polymers, and thus the polyelectrolyte solution becomes semidilute in a wide concentration range where the average distance ξ between polyions is smaller than L_e.[9] It is in this semidilute regime that the counterion condensation, i.e., an accumulation of counterions in the vicinity of a highly charged polyion, has been theoretically predicted.[1,2,10] Various equilibrium properties have been well explained by the condensation theories based on the two-phase model where the counterions are distributed either in the free or in the bound phase. The free counterions contribute to the conductivity (or the activity) while the bound ones to the dielectric properties since they are assumed to be bound but mobile (i.e., polarizable) in the potential produced by the polyion. Thus, the dielectric relaxation spectroscopy of the polyelectrolyte solutions in

* Address correspondence to this author at Fundamental Research Laboratories NEC Co., Miyazaki 4-chome, Miyamae-ku, Kawasaki, Kanagawa 213, Japan.

0024-9297/89/2222-1359$01.50/0

the semidilute regime has been expected to yield detailed information on the dynamical aspect of counterion condensation.

Two kinds of dielectric relaxations with large increments have been observed[11-15] in the kilo- and megahertz ranges, respectively, for semidilute polyelectrolyte solutions with low ionic strength. The low-frequency (LF) relaxation in the kilohertz range depends[12-15] strongly on the molecular weight M_w of the polyelectrolyte while the high-frequency (HF) one in the megahertz range is almost independent of M_w.[12,14-19] The LF relaxation has been attributed to the polarization of bound but mobile counterions along the rodlike polyion axis,[20,21] because of its strong dependence on M_w. This interpretation has many modifications which incorporate the Coulombic interactions between bound counterions,[22,23] the transitional motion of counterions between discrete sites on the polyion,[24,25] the exchange of counterions between the bound and free phases,[26] and the effect of polyion rotation.[27] The HF relaxation, on the other hand, has been explained in terms of two different mechanisms: the counterion polarization along and within a rodlike "subunit" of the polyion[14,15,27] and that perpendicular to the polyion axis.[18,19,28-30] Hence, there remains an apparent controversy on the direction of counterion polarization in the HF relaxation.

Most of these explanations for the LF and HF relaxations are based on the conventional two-phase model. A Poisson–Boltzmann analysis[31,32] using the cell model has shown that all the bound counterions are not accumulated on the polyion surface as implied by the two-phase model, but they are distributed both in the tightly bound phase in the immediate vicinity of the polyion and in the loosely bound phase surrounding the former one, resulting in the spread of bound counterion distribution in the direction vertical to the polyion axis. There are a few theoretical approaches[33,34] which treat the dielectric increment in the LF relaxation with no premise of the two-phase model.

In spite of numerous studies on the statics and dynamics of counterions, how tightly or loosely the counterions are bound to the polyion and how the bound counterions move in the electrostatic potential of the polyion have been still unclear in both experimental and theoretical aspects, allowing the controversies in the interpretations for the LF and HF relaxations.

In this paper, we aim to obtain fundamental information on the counterion dynamics, such as the mobilities and motional directions of the counterions which contribute to the LF and HF relaxations. For this purpose, we employ the frequency-domain electric birefringence (FEB) method where the birefringence response Δn to an external sinusoidal electric field is detected for a series of the field frequencies to obtain the relaxation spectrum of Δn (FEB spectrum).[35-37] FEB spectroscopy is superior to conventional dielectric relaxation spectroscopy in that it enables us to obtain information on the anisotropy in the dielectric relaxation (i.e., on the polarization direction) as well as on the rotational relaxation of the polyion separately from the dielectric relaxation. These features allow us to acquire insights into the counterion dynamics and the polyion conformation, which are reflected in the rotational relaxation of the polyion. FEB spectroscopy is more adequate for the present purpose than a conventional time-domain electric birefringence (TEB) method,[38-42] because the TEB response is less sensitive to anisotropy in the relaxational polarizabilities and requires much more complex analysis compared with the case of FEB.

In the following, we describe the outline of FEB relaxation spectroscopy and the experimental FEB spectra obtained for typical polyelectrolytes in aqueous solutions by using a highly sensitive FEB apparatus. Then we discuss the observed FEB relaxations in relation to counterion dynamics and to polyion conformation.

Frequency-Domain Electric Birefringence Relaxation

To clarify the significance of FEB relaxation spectroscopy, we first describe the relation between the dielectric and the electric birefringence responses of a solution containing rigid molecules with both permanent and induced dipole moments. The rigid molecules include, as a typical example, a rodlike molecule, which is an approximate model for an extended polyion in the solution with low ionic strength.

Dielectric Relaxation. Let us assume that a rigid molecule with arbitrary shape has both permanent dipole moments $\{\mu_{0j}\}$ and complex (i.e., frequency-dependent) electrical polarizabilities $\{\alpha^*_j\}$ in a solution, where the suffix j denotes the principal axis j on the molecular frame (j = 1, 2, 3). When the sinusoidal electric field E_j = Re $\{\hat{E}_j \exp(i\omega t)\}$ with a complex amplitude of $\hat{E}_j$ and an angular frequency of ω is applied to the molecule along its j axis, the total dipole moment μ_j of the molecule along the j axis is given by

$$\mu_j = \mu_{0j} + \mu'_j, \qquad \mu'_j = \mathrm{Re}\,\{\alpha^*_j \hat{E}_j \exp(i\omega t)\}, \quad (j = 1, 2, 3) \tag{1}$$

Here, the "molecular-frame" electrical polarizability α^*_j, which determines the induced dipole moment μ'_j along the j axis, is assumed to be represented by the Debye-type response function written as

$$\alpha^*_j = \frac{\alpha_j}{1 + i\omega\tau_j} + \alpha_{j\infty} \tag{2}$$

where α_j is the polarizability increment (relaxation strength), τ_j the relaxation time of the induced polarization, and $\alpha_{j\infty}$ the polarizability in the high-frequency limit.

The dielectric constant $\Delta\epsilon^*$ of the solution in excess of the solvent contribution is given by an isotropic average of the principal values $\{\tilde{\alpha}^*_j\}$ of the "total" electrical polarizability tensor, which takes into account the rotational motion of the molecule, as

$$\Delta\epsilon^* = c(\tilde{\alpha}^*_1 + \tilde{\alpha}^*_2 + \tilde{\alpha}^*_3)/(3\epsilon_0) \tag{3}$$

where c is the number of solute molecules per unit volume and ϵ_0 the vacuum permittivity. The principal value $\tilde{\alpha}^*_j$ is given by[43]

$$\tilde{\alpha}^*_j = \frac{\mu^2_{0j}/(k_B T)}{1 + i\omega\tau_{rj}} + \frac{\alpha_j}{1 + i\omega\tau'_j} + \alpha_{j\infty} \tag{4}$$

where $k_B T$ is the thermal energy and τ_{rj} is the rotational relaxation time of the molecule with respect to the j axis given as[44]

$$\tau_{r1} = (D_2 + D_3)^{-1}, \qquad \tau_{r2} = (D_3 + D_1)^{-1}, \qquad \tau_{r3} = (D_1 + D_2)^{-1} \tag{5}$$

Here D_j is the rotational diffusion constant around the j axis. In eq 4, τ'_j is the apparent or effective relaxation time of the induced polarization along the j axis, which is given by a harmonic mean of τ_{rj} and the "intrinsic" relaxation time τ_j of the induced polarization along the j axis, as

$$(\tau'_j)^{-1} = (\tau_{rj})^{-1} + (\tau_j)^{-1} \tag{6}$$

The dielectric constant $\Delta\epsilon^*$ in eq 3 is related to $\tilde{\alpha}^*_j$ given by eq 4, in which the first term on the right-hand side represents the orientational (rotational) polarizability due to the permanent dipole moment μ_{0j}, while the second and third are the induced polarizability terms which are de-

rived from α^*_j in eq 2 by taking into account the modulation effect due to the rotational motion of the molecule.

It is seen from eq 6 that when τ_j is much larger than τ_{rj}, the induced polarizability relaxes with τ'_j nearly equal to τ_{rj} and is indistinguishable from the orientational one. Thus, even if the permanent dipole moment μ_{0j} is equal to zero, the dielectric relaxation due to the induced polarizability would appear with the rotational relaxation time τ_{rj} as if the solute molecule has a permanent dipole moment.

On the contrary, if τ_j is much smaller than τ_{rj}, the dielectric relaxation would occur with τ'_j nearly equal to τ_j and the rotational relaxation would not appear when μ_{0j} is zero.

FEB Relaxation. The birefringence induced by a sufficiently weak electric field is a quadratic function of the electric field strength (Kerr's law). Then the birefringence response Δn to the sinusoidal electric field $E = \mathrm{Re}\{\hat{E}\exp(i\omega t)\}$ with an amplitude of $\hat{E}$ small enough consists of dc (static) and 2ω (ac) components, viz., Δn_{dc} and $\Delta n_{2\omega}$, respectively. Correspondingly, the Kerr response K, which is defined as Δn divided by the mean-square value of E, i.e., $|\hat{E}|^2/2$, is written as

$$K \equiv 2\Delta n/|\hat{E}|^2 = K_{dc} + \mathrm{Re}\,[K^*_{2\omega}\exp(i2\omega t)] \quad (7)$$

where K_{dc} corresponds to Δn_{dc} and $K^*_{2\omega}$ ($\equiv K'_{2\omega} - iK''_{2\omega}$) is the complex amplitude corresponding to $\Delta n_{2\omega}$. The FEB response for the same model system as employed in the preceding section was studied in the previous papers,[45,46] and the dc component K_{dc} was given as

$$K_{dc} = \frac{c}{60n\epsilon_0 k_B T}\,\mathrm{Re}\,[(\alpha_1^{op} - \alpha_2^{op})(\tilde{\alpha}^*_1 - \tilde{\alpha}^*_2) + (\alpha_2^{op} - \alpha_3^{op})(\tilde{\alpha}^*_2 - \tilde{\alpha}^*_3) + (\alpha_3^{op} - \alpha_1^{op})(\tilde{\alpha}^*_3 - \tilde{\alpha}^*_1)] \quad (8)$$

where α_j^{op} is the optical polarizability of the molecule along the j axis and n the refractive index of the solution. When ω tends to zero, eq 8 reduces to the well-known expression of the Kerr constant for a static electric field.[47,48] The expression for the TEB response, which corresponds to eq 8, has a much more complex form than eq 8.

Though the electric birefringence is essentially a nonlinear response to the electric field, K_{dc} in eq 8 is a linear function of the real parts of $\tilde{\alpha}^*_j$'s, which characterize the dielectric response as in eq 3. Thus, the measurement of K_{dc} as a function of frequency can be utilized as a kind of dielectric relaxation spectroscopy.

In contrast to conventional dielectric relaxation spectroscopy where the isotropic mean of $\tilde{\alpha}^*_j$ is obtained as in eq 3, each term of K_{dc} in eq 8 is proportional to the difference of $\tilde{\alpha}^*_j$'s, and therefore the K_{dc} spectrum affords us information on the anisotropy in the dielectric properties of solutions. This feature of the K_{dc} spectrum is very useful to assign the molecular mechanism of the observed relaxation, because we can discriminate by the sign of K_{dc} the direction of the electrical polarization which contributes to the relaxation.

For a solution containing rodlike molecules which are assumed to satisfy the relations $\alpha_1^{op} = \alpha_2^{op}$, $\tilde{\alpha}^*_1 = \tilde{\alpha}^*_2$, and $D_1 = D_2 \ll D_3$ (i.e., the 3-axis is regarded as a rod axis), the K_{dc} and $K^*_{2\omega}$ responses are simplified to

$$K_{dc} = \mathrm{Re}\,\{\psi^*\}, \qquad K^*_{2\omega} = \psi^*\phi^* \quad (9)$$

In eq 9, ψ^* and ϕ^* are the response functions which represent the dielectric and rotational relaxations, respectively, and are given as

$$\psi^* \equiv A(\tilde{\alpha}^*_3 - \tilde{\alpha}^*_1), \qquad \phi^* \equiv 1/(1 + 2i\omega\tau_{r3}/3) \quad (10)$$

where A is a frequency-independent constant defined by

$$A \equiv c(\alpha_3^{op} - \alpha_1^{op})/(30n\epsilon_0 k_B T) \quad (11)$$

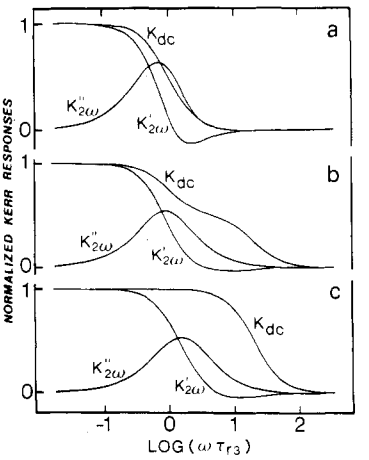

Figure 1. Theoretical FEB spectra calculated from eq 9 and 10 for a molecule with (a) an orientational polarizability alone, (b) a 1:1 mixture of orientational and induced polarizabilities, and (c) an induced polarizability alone. Here, $\tilde{\alpha}^*_3$ alone is taken into account and τ_3/τ_{r3} is assumed to be 20.

It is seen from eq 9 that a simultaneous measurement of K_{dc} and $K^*_{2\omega}$ spectra affords us both ψ^* and ϕ^* separately, from which we can obtain the dielectric relaxation time τ'_3 and the rotational relaxation time τ_{r3}, respectively. Then the intrinsic relaxation time τ_3 of the induced polarization can be evaluated from τ'_3 and τ_{r3} through eq 6. Thus, the simultaneous measurement of K_{dc} and $K^*_{2\omega}$ spectra makes it possible to discriminate between the induced and rotational relaxations. This is another advantage of the FEB spectroscopy over conventional dielectric relaxation spectroscopy.

To illustrate the relation between the FEB spectra and the polarization mechanisms, the theoretical FEB spectra calculated for three typical cases by using eq 9 and 10 are shown in Figure 1 where the contribution of $\tilde{\alpha}^*_3$ alone is taken into account ($\tilde{\alpha}^*_1 = 0$). The molecule is assumed to have orientational polarizability due to the permanent dipole moment μ_{03} alone, i.e., $\mu_{03} \neq 0$ and $\alpha_3 = 0$ (Figure 1a), the mixture of the orientational and induced polarizabilities in equal weight, i.e., $\mu_{03}^2/(k_B T) = \alpha_3 \neq 0$ (Figure 1b), and the induced one alone, i.e., $\mu_{03} = 0$ and $\alpha_3 \neq 0$ (Figure 1c). Here it is assumed that the polarizability $\alpha_{3\infty}$ in the high-frequency limit is zero in all the cases and τ_3 in the cases of Figure 1b,c is an order of magnitude smaller than τ_{r3}.

The K_{dc} spectrum is quite different between parts a and c of Figure 1; the angular frequency ω_{dc}, yielding an inflection point, of the K_{dc} spectrum is equal to $1/\tau_{r3}$ in Figure 1a, while ω_{dc} is given approximately by $1/\tau_3$ in Figure 1c since τ_3 is much smaller than τ_{r3}. The profile of the K_{dc} spectrum is sensitive to both the orientational and the induced polarizations as seen in Figure 1b, where the two relaxations due to both types of polarizations appear.

On the other hand, the angular frequency ω_{ac}, giving the extremum of $K''_{2\omega}$, changes only slightly from $0.69/\tau_{r3}$ in Figure 1a to $1.5/\tau_{r3}$ in Figure 1c. Thus, the $K^*_{2\omega}$ spectrum is almost determined by the rotational relaxation time τ_{r3} and is insensitive to the polarization mechanisms. This makes a clear contrast to the case of the K_{dc} spectrum where ω_{dc} drastically changes by an order of magnitude as in Figure 1a,c.

As an example, the FEB spectra of nonionic solutions of rodlike polymers, i.e., poly(γ-benzyl L-glutamate) (PBLG), in m-cresol are shown in Figure 2 where the observed values of K_{dc}, $K'_{2\omega}$, and $K''_{2\omega}$ are plotted against the electric field frequency f ($=\omega/2\pi$). The PBLG molecule

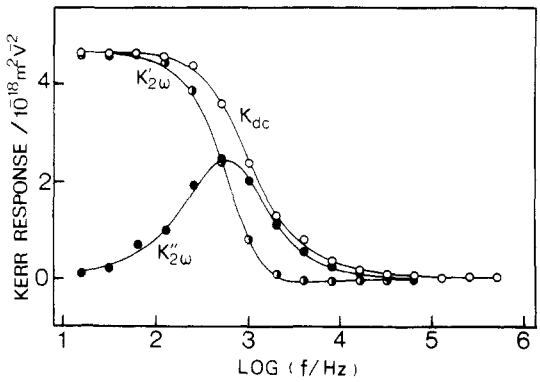

Figure 2. FEB spectra of PBLG solution in dilute regime (0.4 wt %).

in *m*-cresol has an α-helical rodlike conformation which is stabilized by intramolecular hydrogen bonds with a dipole moment aligned approximately parallel to the rod axis, resulting in a large permanent dipole moment μ_{03} of the molecule along the rod axis. In this case, the contribution of μ_{03} to the excess dielectric constant $\Delta\epsilon^*$ of the solution is expected to be overwhelmingly larger than those from μ_{01}, μ_{02}, α_j's, and $\alpha_{j\infty}$'s (j = 1–3), and therefore the PBLG solution would show the FEB spectra similar to Figure 1a.

As is expected, the experimental K_{dc} and $K^*_{2\omega}$ spectra in Figure 2 have nearly the same relaxation frequencies, i.e., K_{dc} has a positive plateau below 100 Hz and relaxes in the vicinity of 1 kHz, where $K''_{2\omega}$ yields an extremum.

These FEB spectra in Figure 2 are well explained in terms of the rotational relaxation due to μ_{03} alone, as shown by the solid curves in the figure which have been obtained by the nonlinear least-squares fitting procedure for the observed values of K_{dc}, $K'_{2\omega}$, and $K''_{2\omega}$ through eq 9, 10, and 4 with the μ_{03} term only. Here, the response functions ψ^* and ϕ^* of the Debye type in eq 9 and 10 have been replaced by empirical ones of Havriliak–Negami type[49] to take into account the distribution of relaxation times.

Experimental Section

The polyelectrolyte samples used in this study are sodium salts of polystyrenesulfonate (NaPSS), (carboxymethyl)cellulose (NaCMC), and deoxyribonucleic acid (NaDNA).

A monodisperse NaPSS sample (Pressure Chem. Co., no. 12) with a molecular weight (M_w) of 4.12×10^5 g and a nominal M_w/M_n ratio of 1.10 was dissolved in pure water (glass-distilled and deionized water) at 4 °C. Then the solution was dialyzed against pure water, passed through a mixed-bed ion exchange resin (IR-120 and IR-45) column, neutralized by addition of a freshly prepared NaOH solution, and used after dilution with pure water. In these procedures, the sample solution was handled under atmospheric nitrogen gas.

A NaCMC sample (Daicel Chem. Ind. Jpn., no. 135) with a degree of substitution (DS) of 1.9 was purified by precipitation from aqueous solution with addition of methanol in the presence of NaOH. Then the NaCMC solution was centrifuged at 20 000 rpm for 3 h to remove its gel fraction and freeze-dried. The molecular weight of the sample was estimated to be 4.3×10^5 g by viscometry in 0.1 M NaCl.[50] The sample solution obtained by dissolving the dried sample in a pure water at 4 °C was subjected to the same procedures as in the case of NaPSS.

A calf thymus NaDNA sample (Sigma Chem. Co., Type V) was dissolved in a BPES buffer containing 6 mM Na_2HPO_4, 2 mM NaH_2PO_4, 1 mM Na_2EDTA, and 0.18 M NaCl under an atmospheric argon gas at 4 °C. The solution was then sonicated at 0 °C with a Branson sonifier and fractionated at 15 °C on an Agarose Gel (Bio-rad, Bio-gel A-15m) column equilibrated before by the same buffer. The fraction with an average molecular weight of 4.7×10^5 g determined by viscometry[51] was used after dialysis against 0.1 mM NaCl.

Table I
Parameters of Polyelectrolyte Samples Used in the FEB Measurement

	10^3C_p, M	$10^{-5}M_w$, g	M_m, g	l_m, nm	n_m	L_c, nm
NaPSS	1.0	4.1	206	0.25	1	500
NaCMC	0.5	4.3	300	0.51	1.9	730
NaDNA	3.2	4.7	614	0.33	2	250

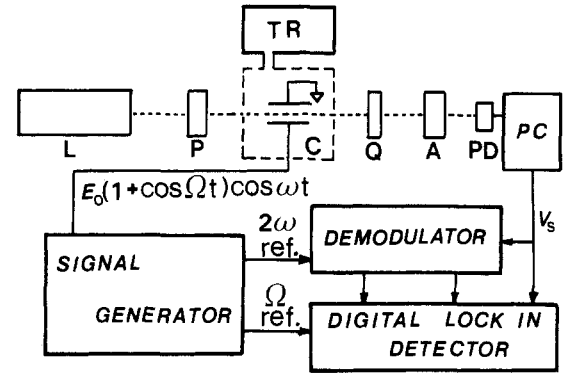

Figure 3. Simplified block diagram of FEB apparatus. L, argon ion laser (514.5 nm); P, Glan-Thompson prism polarizer; C, Kerr cell; Q, quartz quarter-wave plate; A, Rochon prism analyzer; PD, photodiode; PC, photocurrent-to-voltage converter; TR, thermoregulator.

Table I summarizes the polyelectrolyte molecular weight M_w and the polyelectrolyte concentration C_p, which is defined as the concentration of charged sites on the polyions. The latter was determined by potentiometric titration for NaPSS and NaCMC solutions and by UV absorption for NaDNA solution.

Molecular parameters of the polyelectrolytes used are also listed in Table I, where M_m is the monomer molecular weight, l_m the monomer length along the polyion contour, n_m the number of monovalent charges on a monomeric unit, and L_c ($=M_w l_m/M_m$) the polyion contour length. The value of M_m for NaCMC was obtained by assuming that the polymer consists of monomers with a DS of 1 or 2, which yielded an average DS value of 1.9. In the case of NaDNA, a base pair is taken as a monomeric unit whose M_m is an averaged one obtained by assuming a GC content of 42%.

The K_{dc} and $K^*_{2\omega}$ spectra were simultaneously measured in the frequency ranges from 2 Hz to 8.4 MHz for K_{dc} and from 2 Hz to 65 kHz for $K^*_{2\omega}$. We briefly describe the outline of the FEB spectrometry by using a simplified block diagram of the FEB apparatus shown in Figure 3.

In the optical part of the apparatus, an argon ion laser with high intensity and high stability is used to attain an excellent S/N ratio in the birefringence detection. The light from the laser with the wavelength λ equal to 514.5 nm is transmitted through the polarizer, Kerr cell (sample cell), $\lambda/4$ plate, and analyzer with a small offset angle θ from its extinction position. The light intensity I after the analyzer is given by[36]

$$I = \zeta P\{\sin(\delta/2)\sin(2\theta + \delta/2) + \sin^2\theta\} \quad (12)$$

where ζ is the quantum efficiency of photodetection, P the light intensity on the specimen, and δ the optical phase retardation which is proportional to the electric birefringence Δn as $\delta = 2\pi l\Delta n/\lambda$ (l, the light path length of the Kerr cell). Equation 12 can be rewritten for $|\delta| \ll \theta \ll 1$ as

$$I = \zeta P(\theta^2 + \theta\delta) \quad (13)$$

where the second term on the right-hand side is proportional to Δn.

A signal generator synthesizes the amplitude-modulated electric field $E = E_0(1 + \cos\Omega t)\cos\omega t$, satisfying the condition $\Omega \ll \omega$. This electric field applied to the Kerr cell induces the birefringence signal Δn in which the K_{dc} and $K^*_{2\omega}$ components, which have been located at dc and 2ω under an unmodulated sinusoidal field, are shifted to the angular frequencies Ω and $2\omega \pm \Omega$, respectively. This modulation technique for shifting the signal frequencies makes possible the Δn measurement with a high S/N by using a digital lock-in detector[36] system as described in the following.

Table II
Best-Fitting Parameters for FEB Spectra of Polyelectrolyte Solutions

	$10^{17}K_L$, $(m/V)^2$	$10^{17}K_H$, $(m/V)^2$	τ_R, ms (a_R, b_R)	τ_L, ms (a_L, b_L)	τ_H, μs (a_H, b_H)
NaPSS	27	−2.6	1.7 (1.0, 1.0)	0.19 (0.92, 0.95)	0.14 (1.0, 0.93)
NaCMC	−9.5	1.2	3.2 (1.0, 0.90)	0.64 (0.82, 0.83)	0.32 (1.0, 0.82)
NaDNA	3.7	−1.6	0.18 (1.0, 1.0)	0.019 (0.83, 0.99)	0.043 (1.0, 1.0)

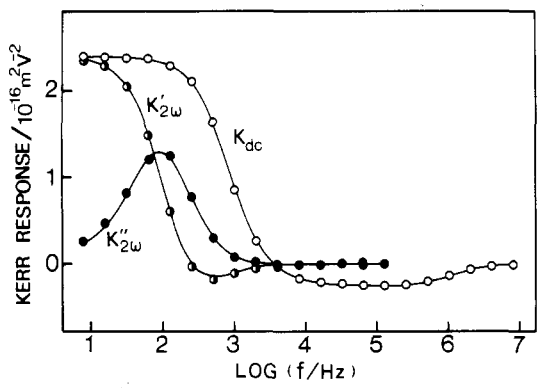

Figure 4. FEB spectra of NaPSS solution. Solid curves are those obtained from eq 14–16 by using the best-fitting parameters listed in Table II.

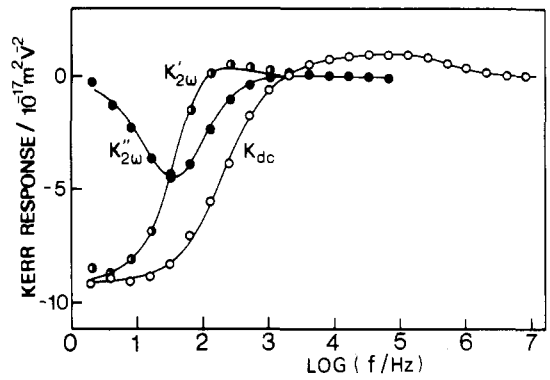

Figure 5. FEB spectra of NaCMC solution. The best-fitting parameters for solid curves are listed in Table II.

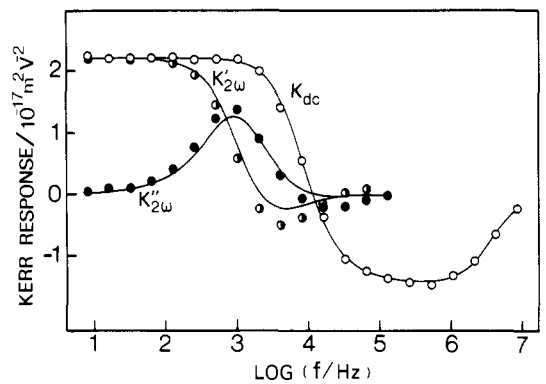

Figure 6. FEB spectra of NaDNA solution. The best-fitting parameters for solid curves are listed in Table II.

The frequency-shifted Δn signal is detected by a photodiode as a photocurrent signal and converted by a photocurrent-to-voltage converter into the voltage signal V_s. In a digital lock-in detector system, the Ω component in V_s, which is proportional to K_{dc}, is detected by a demodulation with a reference wave of $\cos \Omega t$, and the components in V_s, which are located at $2\omega \pm \Omega$ and proportional to $K^*_{2\omega}$, are detected by a two-step demodulation procedure: the V_s signal is first demodulated by a two-phase demodulator with reference waves of $\cos 2\omega t$ and $\sin 2\omega t$ into two Ω components proportional to $K'_{2\omega}$ and $K''_{2\omega}$, respectively, which are subsequently detected by a demodulation with a reference wave of $\cos \Omega t$.

This detection method allows us to detect a very small Δn signal of the order of 10^{-13} with $l = 10^{-2}$ m. Hence, the amplitude of applied electric field was easily reduced to less than 2 kV/m in the present study to minimize undesirable effects such as the joule heating of the sample solution. The temperature of the Kerr cell was kept at 13.0 °C.

Results and Analysis

In Figure 4 are shown the FEB spectra of a NaPSS solution with no added salt. The K_{dc} spectrum exhibits a positive plateau below ca. 100 Hz, decreases markedly in the vicinity of ca. 1 kHz (the low-frequency (LF) relaxation), and changes its sign from positive to negative at ca. 4 kHz. Further increase in the frequency results in the decrease of absolute values of K_{dc} toward zero value in the vicinity of ca. 1 MHz (the high-frequency (HF) relaxation) after a negative plateau region. On the other hand, the $K''_{2\omega}$ spectrum shows an extremum at ca. 100 Hz, which is an order of magnitude lower than the LF relaxation frequency.

The FEB spectra were analyzed by using the nonlinear least-squares method. In this analysis, the rodlike model was employed for the polyion which takes an extended conformation in the semidilute solution with no or little amount of added salt. Then we were led to the following expressions based on eq 9 and 10

$$K_{dc} = \mathrm{Re}\,(\psi^*), \qquad \psi^* = K_L\phi^*_L + K_H\phi^*_H \tag{14}$$

$$K^*_{2\omega} = \psi^*\phi^*_R \tag{15}$$

where the response functions of Havriliak–Negami type[49]

$$\phi^*_k = 1/\{1 + (i\omega\bar{\tau}_k)^{b_k}\}^{a_k}, \qquad (k = L, H, \text{and } R) \tag{16}$$

were used instead of Debye-type functions to take into account the distribution of relaxation times. In eq 14 and 16, K, $\bar{\tau}$, a, and b with the subscript k denote the electric birefringence increment (relaxation strength), the nominal relaxation time, the asymmetry parameter, and the broadness parameter, respectively ($0 < a, b \leq 1$). The subscripts L, H, and R stand for LF, HF, and rotational relaxations, respectively. The contribution of nonrelaxational, anisotropic polarizability $\alpha_{3\infty} - \alpha_{1\infty}$ to ψ^* was neglected because it was much smaller than the relaxational parts as seen in Figure 4.

The solid curves of K_{dc}, $K'_{2\omega}$, and $K''_{2\omega}$ in Figure 4 were obtained by the best fitting to the data points using eq 14–16: The nonlinear least-squares fitting to the observed K_{dc} data was performed iteratively by using a linearized form of ψ^* in eq 14 for each step. Then, ϕ^*_R was evaluated by the nonlinear least-squares fitting of eq 15 to the observed $K^*_{2\omega}$ data, where ψ^* determined by the first fitting was used.

Figure 5 shows the FEB spectra of NaCMC solution with no added salt, where K_{dc} exhibits a frequency dependence quite similar to that of NaPSS solution except that its sign is just opposite to that in the case of NaPSS; i.e., the electric birefringence increments K_L and K_H of NaCMC solution are negative and positive, respectively. Figure 6 shows the FEB spectra of NaDNA solution with 0.1 mM NaCl, where the relaxation profile is again quite similar to the case of NaPSS solution. The solid curves for K_{dc}, $K'_{2\omega}$, and $K''_{2\omega}$ in Figures 5 and 6 are those obtained by the same fitting procedure as in the case of NaPSS.

Table III
Molecular Parameters of LF and HF Relaxations

	LF		HF	
	τ_3, ms	$10^{11}D_{c3}^{exp}$, m^2/s	d_0, nm	ξ, nm
NaPSS	0.21	9.8	56	82
NaCMC	0.74	6.0	83	110
NaDNA	0.02	26.0	31	56

As shown in Figures 4–6, the polyelectrolyte solutions exhibit essentially the same profile of the FEB spectra consisting of the LF, HF, and rotational relaxations. The relaxation parameters thus obtained are listed in Table II where τ_k is the average relaxation time given as the reciprocal of the angular frequency ω_k yielding the extremum of the imaginary part of relaxation term represented by ϕ^*_k (k = L, H, and R).

According to Table II, the values of a_k and b_k (k = L, H, and R) are all larger than 0.80, indicating that either relaxation has a narrow distribution of relaxation times. The values of a_L and b_L are larger than 0.9 for NaPSS and less than 0.9 for NaCMC, which indicates τ_L has a broader distribution in the case of NaCMC than in the case of NaPSS. In the case of NaDNA, an agreement between the data points and the best-fitting curve of $K^*_{2\omega}$ is insufficient, although a_R and b_R are obtained as 1.0.

Discussion

The analysis in the preceding section has shown that the FEB spectra of the polyelectrolyte solution are described by three relaxation modes with different time scales, i.e., the LF, HF, and rotational relaxation modes. The LF and HF relaxations in the K_{dc} spectrum are identified by their frequency positions with the ones already found by dielectric relaxation spectroscopy.[3,11-15] The dielectric LF relaxation has been ascribed from its strong molecular weight dependence to the counterion polarization along the polyion axis (3-axis). This implies that the LF relaxation in the K_{dc} spectrum corresponds to $\tilde{\alpha}^*_3$ in the expression of ψ^* given by eq 10. Then the sign of K_H which is found to be opposite to that of K_L indicates that the HF relaxation corresponds to $\tilde{\alpha}^*_1$; i.e., the polarization direction of the HF relaxation is vertical to the polyion axis. In the following, we discuss separately the three relaxation modes in the polyelectrolyte solution.

LF Relaxation. The LF relaxation appears in K_{dc} at a frequency that is 1 order of magnitude higher than the rotational relaxation in $K^*_{2\omega}$. This implies that the LF relaxation time is mainly determined by the relaxation time of the induced polarizability α_3; i.e., the effect of the rotational modulation on the LF relaxation time as given in eq 6 is of minor importance. Therefore, the interpretation[52,53] that the LF relaxation is due to the quasi-permanent dipole moment arising from the counterion polarization with a relaxation time slower than the rotational one is inadequate in the present case. The observed LF relaxation time not very different from the rotational one predicts, in the case of TEB, a marked dip response upon the sudden reversal of the electric field polarity, which has been actually observed for a NaPSS solution.[54]

The LF relaxation time τ_L ($=\tau'_3$) is given by eq 6 as the harmonic mean of the intrinsic relaxation time τ_3 of counterion polarization along the polyion axis and the rotational relaxation time τ_{r3} which is equal to $3\tau_R/2$ as seen from eq 10, i.e.

$$(\tau_L)^{-1} = (3\tau_R/2)^{-1} + (\tau_3)^{-1} \quad (17)$$

The value of τ_3 calculated by using eq 17 from the observed values of τ_L and τ_R is listed in Table III, which shows that $\tau_L \simeq \tau_3$; i.e., τ_L is mostly determined by τ_3.

The value of τ_3 can be theoretically estimated as

$$\tau_3 = L_3^2/D_{c3} \quad (18)$$

where D_{c3} and L_3^2 are the diffusion constant and the mean-square diffusion distance, respectively, of bound counterions along the polyion axis. If the counterions are assumed to move in a square well potential[20] with a length of L_0, then we can replace L_3^2 in eq 18 by $L_0^2/12$, i.e.

$$\tau_3 = L_0^2/(12D_{c3}) \quad (19)$$

The upper bound value of D_{c3} is obtained from the observed value of τ_3 through eq 19 by replacing L_0 with its upper bound value L_c (the polyion contour length) and is listed in Table III as D_{c3}^{exp}, which is found to be an order of magnitude smaller than the diffusion constant D_0 (=1.22 $\times 10^{-9}$ m^2/s) of Na^+ ion in a free medium.

The value of D_{c3}^{exp} smaller than D_0 is not explainable by the effects of the Coulombic repulsive interactions between bound counterions[22,23] or the exchange between the bound and free counterions[26] since these effects are expected, to the contrary, to increase D_{c3}.

This slow diffusion process of bound counterions suggests that the LF relaxation may be ascribed to the motion of the counterions in the immediate vicinity of the polyion, where the counterions are densely distributed and tightly bound to the polyion in the electrical potential trough produced by the polyion charges. The translational diffusion of these tightly bound counterions along the polyion would be slowed down by successive potential troughs near the charged sites on the polyion.[55-57] In this case, the tightly bound counterions have to move along the polyion contour and thus L_0 can be equated with L_c.

To summarize, the LF relaxation arises from an induced polarizability due to the counterion motion along the polyion axis. The translational diffusion constant of these counterions is smaller than that in a free medium and hence tightly bound counterions in the immediate vicinity of the polyion seem to be responsible for the LF relaxation.

HF Relaxation. The sign of K_H opposite to that of K_L has led us to the conclusion that the polarization direction in the HF relaxation should be perpendicular to that in the LF relaxation and hence vertical to the polyion axis. Then a model that assumes the polarization direction parallel to the polyion axis, the "subunit" model for instance, is inadequate to explain the HF relaxation. The HF relaxation is ascribable to the induced polarizability α_1 due to the counterion motion vertical to the polyion axis.

The induced polarizability α_j due to the counterion motion along the j axis is in general proportional to the product of the number of counterions n_j which contributes to α_j and the mean-square diffusion length L_j^2 along the j axis, i.e., $\alpha_j \propto n_j L_j^2$. Then the ratio α_1/α_3 is given by

$$\alpha_1/\alpha_3 = (n_1 L_1^2)/(n_3 L_3^2) \quad (20)$$

If n_1 is assumed to be of the same order of magnitude as n_3, then the ratio of L_1^2/L_3^2 is estimated from eq 20 to be in the range 0.1–0.4 by using the observed ratio of K_H/K_L which can be equated with α_1/α_3. This indicates that the diffusion distance L_1 vertical to the polyion axis is much larger than the polyion diameter. Then, in contrast to the LF relaxation which has been ascribed to the tightly bound counterions in the immediate vicinity of the polyion, the HF relaxation is attributable to the loosely bound counterions which surround the tightly bound ones and are subject to the electrostatic potential effectively shielded (i.e., weakened) by the tightly bound counterions. This mechanism for the HF relaxation is consistent with the fact that the HF relaxation time τ_H observed in the dielectric measurement is almost independent of M_w, since

Table IV
Molecular Parameters of Rotational Relaxation

	κ^{-1}, nm	L_e, nm	L_i, nm	L_p, nm	L_p/L_c	$(\langle R^2\rangle)^{1/2}$, nm	$(\langle R^2\rangle)^{1/2}/L_c$	L_a, nm	L_a/L_c	cL_a^3
NaPSS	23	185	1[a]	186	0.37	350	0.70	430	0.86	25
NaCMC	31	335	16[b]	351	0.48	545	0.75	530	0.73	16
NaDNA	14	66	50[c]	116	0.46	185	0.74	190	0.76	9

[a] Reference 60. [b] Reference 5. [c] Reference 61.

the loosely bound counterions would be insensitive to the polyion rotation around the 3 axis. This implies that τ_H is equal to the intrinsic relaxation time τ_1 of the counterion polarization vertical to the polyion axis.

By assuming an equation for τ_1 similar to eq 18 for τ_3, the ratio τ_1/τ_3 is given by

$$\tau_1/\tau_3 = (D_{c3}L_1^2)/(D_{c1}L_3^2) \quad (21)$$

where D_{c1} is the diffusion constant of the counterion in the direction vertical to the polyion axis. If we assume $D_{c1} = D_0$ and $\tau_1 = \tau_H$, which would be valid for the HF relaxation due to the loosely bound counterions, the ratio L_1^2/L_3^2 is estimated from eq 21 to be ca. 0.01 by substituting the value of D_{c3}^{exp} into D_{c3}. If a square well potential with a diameter of d_0 is assumed for the motion of the loosely bound counterions in the direction vertical to the polyion axis, the mean-square diffusion length L_1^2 is given as $d_0^2/8$ and thus the value of d_0 is evaluated from the above ratio L_1^2/L_3^2 with $L_3^2 = L_c^2/12$ as listed in Table III, which shows again that d_0 is much larger than the polyion diameter ($\simeq$1 nm). The result that the ratio L_1^2/L_3^2 estimated from K_H/K_L is larger than that from τ_1/τ_3 may suggest that n_1 is larger than n_3.

In the cell model[31,32,58] where each polyion is surrounded by a cylindrical free volume, the d_0 above estimated is expected to be an average diameter of the distribution of the loosely bound counterions. This diameter should be smaller than the diameter of the cylindrical free volume, namely, the average interpolyion distance (or the correlation length) ξ in the semidilute regime given approximately by

$$c\xi^2 L_c \simeq 1 \quad (22)$$

where c is the number of polyions per unit volume and is given by $c = (M_m C_p N_{AV})/(M_w n_m)$ with the Avogadro number N_{AV}. As listed in Table III, the value of ξ estimated from eq 22 is a little larger than d_0 but of the same order as d_0 and shows an approximate proportionality to d_0. This result seems to support the above HF relaxation mechanism due to the loosely bound counterions which spread over the cylindrical free volume in the semidilute regime. It is to be noted here that the HF relaxation has been related with the correlation length ξ from a viewpoint quite different from the "subunit" model, where ξ is assumed to be the length of the "subunit" measured along the polyion contour.[3,9]

The mean residence time t_r defined by the time for the counterion to escape from the polyion surface to the cylindrical free volume surface was theoretically treated[59] on the basis of the Poisson–Boltzmann formalism for the cell model and compared with the observed data for the dielectric HF relaxation time.[30] The calculated value of t_r for a NaPSS solution of 10^{-3} M was 5.6×10^{-6} s (Table V, ref 59), an order of magnitude larger than the present result for the NaPSS solution ($\tau_H = 1.4 \times 10^{-7}$ s).

To summarize, the HF relaxation in the semidilute regime is found to arise from the induced polarization perpendicular to the polyion axis, which is ascribable to the motion of the loosely bound counterions vertical to the polyion axis.

Rotational Relaxation. We have analyzed the observed FEB relaxation spectra by assuming a rodlike conformation of the polyion. In this section, we discuss the polyion conformation more in details by taking into account the effect of electrical persistence length L_e and estimate the apparent rod length L_a of the polyion from the observed value of the rotational relaxation time τ_{r3}.

The total persistence length L_p of the polyion is given by a sum of intrinsic persistence length L_i and L_e, i.e., $L_p = L_i + L_e$. In the present case, the average separation of charges d_m ($=l_m/n_m$) along the polyion is less than the Bjerrum length l_B ($=e^2/(4\pi\epsilon_0\epsilon k_B T)$; e is the elementary charge, ϵ is the relative permittivity of water), and thus L_e is given by[6]

$$L_e = 1/(4\kappa^2 l_B) \quad (23)$$

where κ^2 is the square of Debye parameter defined as

$$\kappa^2 = 4\pi l_B N_{AV}(2C_s + d_m C_p/l_B) \quad (24)$$

Equation 24 takes into account the contribution of the salt concentration C_s as well as that of the free counterion concentration $d_m C_p/l_B$ which is derived from the condensation theories. The value of L_e calculated from eq 23 is listed in Table IV together with the value of L_i in the literatures.[5,60,61] The value of L_i for NaPSS, which is expected from its chemical structure to be much smaller than L_i for NaCMC and NaDNA, is approximately given by L_i ($\simeq$1 nm) for atactic polystyrene.[60]

The ratio L_p/L_c is not far from unity as shown in Table IV, suggesting that the polyions used in the present study have an extended conformation. As a measure of the polymer extension, we may use the ratio of the root-mean-square end-to-end distance $(\langle R^2\rangle)^{1/2}$ to L_c, which is given by[62]

$$(\langle R^2\rangle)^{1/2}/L_c = [2(u - 1 + e^{-u})]^{1/2}/u \quad (25)$$

where $u = L_c/L_p$. As listed in Table IV, the value of $(\langle R^2\rangle^{1/2})/L_c$ evaluated from eq 25 is larger than 0.7. This implies again an extended conformation of the polyion which may be approximated by a rodlike conformation as an average.

The apparent rod length L_a of the polyion is estimated as follows. If we assume the polyion rotation with the free rotational diffusion constant D_1 given by[63,64]

$$D_1 = \{3k_B T(\ln (L_a/a) - \gamma)\}/(\pi\eta L_a^3) \quad (26)$$

the rotational relaxation time τ_{r3} is related to D_1 as

$$\tau_{r3} = 1/(2D_1) \quad (27)$$

where a is an apparent rod radius, γ a correction term for the end effects, and η the solvent viscosity (=1.2 cP). In Table IV are listed the value of L_a obtained from eq 26 and 27 by using the observed value of τ_{r3} and Broersma's γ,[63] which is weakly dependent on L_a/a with a = 1 nm (the value of L_a thus obtained is insensitive to the value of a). Then the value of L_a/L_c, which is another measure of the polyion extension, is found to be larger than 0.7 as listed in Table IV, also indicating the extended conformation of the polyion.

The agreement between two kinds of extension parameters $(\langle R^2\rangle)^{1/2}/L_c$ and L_a/L_c is satisfactory in the cases of NaCMC and NaDNA but insufficient for NaPSS. This discrepancy may be ascribed to the entanglement effect of the polyions, which should be taken into account in the estimation of L_a, since the value of cL_a^3 (Table IV), which is a characteristic parameter of the entanglement effect, is the largest in the case of the NaPSS solution.

Since the rotational motion of the polyion in the semidilute regime is hindered by the surrounding polyions, the rotational diffusion constant D_r becomes smaller than D_1 for the dilute limit. Therefore, the above treatment using D_1 instead of D_r as in eq 27 results in an underestimation of D_1 and hence an overestimation of L_a. As is known,[65-67] the entanglement effects of rodlike molecules with the rod length L_a are well described in terms of the parameter cL_a^3. The recent studies on the entanglement effect of rodlike molecules in a wide range of concentration[68,69] show us that the ratio D_r/D_1 is estimated to be ca. 0.5 for $cL_a^3 = 25$. Then we have a value of D_1 twice as large as that used above. This larger value of D_1 yields $L_a/L_c \simeq 0.7$, which is in good agreement with the value of $(\langle R^2\rangle)^{1/2}/L_c$ for the NaPSS solution.

To summarize, the apparent rod length of the polyion, which is estimated from the observed rotational relaxation time, is consistent with a large extension of the polyion evaluated from the total (i.e., electrical plus intrinsic) persistence length.

In conclusion, FEB spectroscopy has been found to be a useful tool for clarifying the details of the dynamics of the counterions as well as polyions in the polyelectrolyte solution, since it affords information on both the anisotropic polarizability and the rotational diffusion constant of the polyion surrounded by the counterions. The present FEB study on polyelectrolyte solutions has revealed that, under the influence of the electrostatic potential due to the highly charged polyion with an extended conformation in the semidilute regime, two kinds of polarizations of bound counterions take place in different directions and time scales: the polarization of tightly bound counterions along the polyion axis in the lower frequency range and that of loosely bound counterions vertical to the polyion axis in the higher frequency range.

Acknowledgment. This work was partly supported by the Grant-in-Aid from the Ministry of Education, Science and Culture of Japan.

Registry No. NaPSS, 9080-79-9; NaCMC, 9004-32-4.

References and Notes

(1) Oosawa, F. *Polyelectrolytes*; Marcel Dekker: New York, 1971.
(2) Manning, G. S. *Q. Rev. Biophys.* **1978**, *11*, 179.
(3) Mandel, M.; Odijk, T. *Annu. Rev. Phys. Chem.* **1984**, *35*, 75.
(4) Odijk, T. *J. Polym. Sci., Polym. Phys. Ed.* **1977**, *15*, 477.
(5) Skolnick, J.; Fixman, M. *Macromolecules* **1977**, *10*, 944.
(6) Odijk, T.; Hoowaart, A. C. *J. Polym. Sci., Polym. Phys. Ed.* **1978**, *16*, 627.
(7) Le Bret, M. *J. Chem. Phys.* **1982**, *76*, 6243.
(8) Fixman, M. *J. Chem. Phys.* **1982**, *76*, 6346.
(9) Odijk, T. *Macromolecules* **1979**, *12*, 688.
(10) Ramanathan, G. V.; Woodbury, C. P., Jr. *J. Chem. Phys.* **1982**, *77*, 4133.
(11) Mandel, M.; Jenard, A. *Trans. Faraday Soc.* **1963**, *59*, 2158, 2170.
(12) Minakata, A.; Imai, N. *Biopolymers* **1972**, *11*, 329.
(13) Minakata, A. *Biopolymers* **1972**, *11*, 1567.
(14) van der Touw, F.; Mandel, M. *Biophys. Chem.* **1974**, *2*, 231.
(15) Müller, G.; van der Touw, F.; Zwolle, S.; Mandel, M. *Biophys. Chem.* **1974**, *2*, 242.
(16) Sachs, S. B.; Raizel, A.; Eisenberg, H.; Katchalsky, A. *Trans. Faraday Soc.* **1969**, *65*, 77.
(17) van Beek, W. M.; Odijk, T. J.; van der Touw, F.; Mandel, M. *J. Polym. Sci.* **1976**, *A14*, 773.
(18) Ito, K.; Ookubo, N.; Hayakawa, R. *Rep. Prog. Polym. Phys. Jpn.* **1986**, *29*, 83.
(19) Ito, K.; Yagi, A.; Ookubo, N.; Hayakawa, R. *Macromolecules*, to appear.
(20) Mandel, M. *Mol. Phys.* **1961**, *4*, 489.
(21) Takashima, S. *Adv. Chem. Ser.* **1967**, *63*, 232.
(22) Oosawa, F. *Biopolymers* **1970**, *9*, 677.
(23) Manning, G. *Biophys. Chem.* **1978**, *9*, 65.
(24) Minakata, A.; Imai, N.; Oosawa, F. *Biopolymers* **1972**, *11*, 347.
(25) Warashina, A.; Minakata, A. *J. Chem. Phys.* **1973**, *58*, 3743.
(26) van Dijk, W.; van der Touw, T.; Mandel, M. *Macromolecules* **1981**, *14*, 792, 1554.
(27) van der Touw, F.; Mandel, M. *Biophys. Chem.* **1974**, *2*, 218.
(28) Minakata, A. *Ann. N.Y. Acad. Sci.* **1977**, *303*, 107.
(29) Wesenberg, G. E.; Vaughan, W. E. *Biophys. Chem.* **1983**, 381.
(30) Cametti, C.; Biasio, A. D. *Macromolecules* **1987**, *20*, 1579.
(31) Guëron, M.; Weisbuch, G. *Biopolymers* **1980**, *19*, 353.
(32) Guëron, M.; Weisbuch, G. *J. Phys. Chem.* **1979**, *83*, 1991.
(33) Fixman, M. *Macromolecules* **1980**, *13*, 711.
(34) Rau, D. C.; Charney, E. *Biophys. Chem.* **1981**, *14*, 1.
(35) Wilkinson, R. S.; Thurston, G. B. *Biopolymers* **1973**, *15*, 1555.
(36) Ookubo, N.; Mori, Y.; Hayakawa, R.; Wada, Y. *Jpn. J. Appl. Phys.* **1980**, *19*, 2271.
(37) Ookubo, N.; Hayakawa, R.; Wada, Y. *Jpn. J. Appl. Phys.* **1981**, *20*, 801.
(38) Krause, S.; O'Konski, C. T. In *Molecular Electro-Optics*; Krause, S., Ed.; Plenum: New York, 1981.
(39) Elias, J. G.; Eden, D. *Macromolecules* **1981**, *14*, 410.
(40) Tricot, T.; Houssier, C. *Macromolecules* **1982**, *15*, 854.
(41) Szabo, A.; Haleem, M.; Eden, D. *J. Chem. Phys.* **1986**, *85*, 7472.
(42) Wijmenga, S. S.; van der Touw, F.; Mandel, M. *Macromolecules* **1986**, *19*, 1760.
(43) South, G. P.; Grant, E. H. *Biopolymers* **1973**, *12*, 1937.
(44) Perrin, F. *J. Phys. Radium* **1934**, *5*, 497.
(45) Hayakawa, R. *Polym. Prep. Jpn.* **1981**, *33*, 1796.
(46) Hayakawa, R.; Ookubo, N. *J. Chem. Phys.*, to appear.
(47) LeFevre, C. G.; LeFevre, R. J. W. *Rev. Pure Appl. Chem.* **1959**, *63*, 1558.
(48) Holcomb, D. H.; Tinoco, I., Jr. *J. Phys. Chem.* **1963**, *67*, 2691.
(49) Havriliak, S.; Negami, S. *J. Polym. Sci.* **1966**, *C14*, 99.
(50) Sitaramaiah, G.; Goring, D. A. I. *J. Polym. Sci.* **1962**, *58*, 1107.
(51) Reinert, K. E.; Straussburger, J.; Triebel, H. *Biopolymers* **1971**, *10*, 2619.
(52) Sakamoto, M.; Kanda, H.; Hayakawa, R.; Wada, Y. *Biopolymers* **1976**, *15*, 879.
(53) Sakamoto, M.; Hayakawa, R.; Wada, Y. *Biopolymers* **1978**, *17*, 1507; **1979**, *18*, 2769; **1980**, *19*, 1039.
(54) Ookubo, N.; Teraoka, I.; Hayakawa, R. *Ferroelectrics*, in press.
(55) Lifson, S.; Jackson, J. L. *J. Chem. Phys.* **1962**, *36*, 2410.
(56) Jackson, J. L.; Coriel, S. R. *J. Chem. Phys.* **1963**, *38*, 959.
(57) Morita, A.; Watanabe, H. *Macromolecules* **1984**, *17*, 1545.
(58) Katchalsky, A. *Pure Appl. Chem.* **1971**, *26*, 327.
(59) Halle, B.; Wennerstrom, H.; Piculell, L. *J. Phys. Chem.* **1984**, 2482.
(60) Flory, P. J. *Statistical Mechanics of Chain Molecules*; John Wiley & Sons: New York, 1969.
(61) Godfrey, J. E.; Eisenberg, H. *Biophys. Chem.* **1976**, *5*, 301.
(62) Yamakawa, H. *Modern Theory of Polymer Solutions*; Harper & Row: New York, 1971.
(63) Broersma, S. *J. Chem. Phys.* **1960**, *32*, 1626, 1632.
(64) Nakajima, H.; Wada, Y. *Biopolymers* **1978**, *17*, 2291.
(65) Doi, M. *J. Phys. Paris* **1975**, *36*, 607.
(66) Doi, D.; Edwards, S. F. *J. Chem. Soc., Faraday Trans. 2* **1978**, *74*, 560, 918.
(67) Doi, M.; Edwards, S. F. *The Theory of Polymer Dynamics*; Clarendon Press: Oxford, 1986.
(68) Mori, Y.; Ookubo, N.; Hayakawa, R.; Wada, Y. *J. Polym. Sci., Polym. Phys. Ed.* **1982**, *20*, 2111.
(69) Teraoka, I.; Ookubo, N.; Hayakawa, R. *Phys. Rev. Lett.* **1985**, *24*, 2712.